

Analysis Of A Reacting Laminar Flow In A Saturated Porous Media Channel With Two Distinct Horizontal Permeable Walls

Amumeji, OlaseniTaiwo

Department of Mathematical Sciences

Ondo State University of Science and Technology, Okitipupa, NIGERIA

Abstract: An analytical study of momentum and heat transfer characteristics with/without suction/blowing of a reacting laminar flow in a horizontal channel filled with saturated porous media with both isothermal and isoflux boundary conditions has been carried out. The problem was studied under the Arrhenius reaction, viscous dissipation and suction. The dimensional ordinary differential equations governing the flow and the heat transfer characteristics are converted into dimensionless ordinary differential equations.

The system is solved analytically using the method of undetermined coefficients and the series solution through perturbation method. Details of velocities and temperature fields for various values of the governing parameters of the problems are presented. The contoured graphical results plotted with the numerical results display the effects of various flow parameters such as the suction/injection Reynolds number, Re , Darcy number, Da , ratio of the effective viscosity of porous region to the viscosity of the fluid, M , Brinkman number, Br , Peclet number, Pe and the Frank-Kamenetskii parameter, β due to Arrhenius kinetic term on the velocity and temperature profiles with the two distinct wall conditions.

Keywords: isoflux/isothermal, laminar flow, porous medium, reacting fluid, suction/injection.

| | | | | |
|---------------|---|------------------------------------|-----------|--|
| Nomenclature | | R | - | gas rate constant |
| | | Re | - | suction/injection Reynolds number |
| a | - | channel width | | |
| A_0^n | - | Pre-exponential factor | T_0 | - wall temperature |
| Br | - | Brinkman number | T | - absolute temperature |
| Da | - | Darcy number | u | - dimensionless fluid velocity |
| ε | - | activation energy parameter | \bar{u} | - fluid velocity |
| E | - | activation energy | V_0 | - suction velocity |
| F | - | specific heat at constant pressure | \bar{x} | - axial coordinate |
| | | | y | - dimensionless transverse coordinate |
| | | | \bar{y} | - transverse coordinate |
| G | - | applied pressure gradient | β | - Frank-Kamenetskii parameter |
| k | - | fluid thermal conductivity | ρ | - fluid density |
| K | - | permeability | μ | - fluid viscosity |
| M | - | ratio of viscosities | μ_e | - effective viscosity in the Brinkman term |
| Pe | - | Péclet number | θ | - dimensionless temperature |
| q | - | fluid flux rate | | |
| Q | - | heat of reaction | | |

I. Introduction

Flow through porous media have been extensively studied due to its relevance in various technological applications such as heat transfer associated with the nuclear waste disposal, prevention of sub soil water pollution, solid matrix heat exchanger, thermal insulation, heat recovery from geothermal energy system, storage systems of the agricultural products e.t.c. The mechanisms of the mixed convection in the porous media have significant applications in the utilization of geothermal energy. The books of Nield and Benjan [22] and Ingham and Pop [12] have extensively studied the works majored in this area.

The majority of the studies on convection heat transfer in porous media are based on Darcy's law, (Darcy, [8]). The accuracy of these results is restricted to specific ranges of Darcy and Reynolds numbers.

Vafai and Tien [31] investigated and revealed the importance of Brinkman number and Forchheimer terms in forced convection over a flat plate and presented the resulting error in heat transfer coefficient when the viscous and inertial terms are negligible. Similarly, a study was reported by Ranganathan and Viskanta [27] revealing the wall and inertia effects in mixed convection flow over flat plate. In the works of Tong and Subramaniam [30] and that of Lauriat and Prasad, [17], it was indicated that in natural convection flow, wall effect is negligible for Darcy number below than 10^{-5} . Vermal and Chauhan [32] solved unsteady fluid flow through a circular naturally permeable tube surrounded by a porous material. Fand *et al.* [10] carried out an experimental investigation of free convection from a horizontal circular cylinder embedded in a porous medium and reported that deviations from the Darcy's law occur when the Reynolds number based on the pore diameter exceeds 1-10, thus, the non-Darcy flow situation is more likely to prevail when the Rayleigh number is sufficiently high and that the boundary layer approximations are relevant. Paul *et al.* [25] in their paper titled transient free convective flow in a channel with constant temperature and constant heat flux on walls studied the transient free convective flow in a vertical channel having a constant temperature and constant heat flux on the channel walls.

Dasset *et al.* [9] studied the unsteady free convection and mass transfer boundary layer flow past an accelerated infinite vertical porous flat plate with suction when the plate accelerates in its own plane. The work showed that the flow phenomenon was characterized with the help of flow parameters such as suction parameter, porosity parameter, Grashof number, Schmidt number and Prandtl number and their effects on velocity, temperature and concentration distributions are also studied.

Mishra *et al.* [21] obtained the solution of fully developed free and forced convection flow in a porous medium bounded by two vertical walls when there is a uniform axial temperature variation along the walls. Cheng [7] investigated the mixed convection flow about horizontal impermeable surfaces in a saturated porous medium with aiding external flows. Mazumder [20] studied the dispersion of solute in natural convection flow through a vertical channel with a linear axial temperature variation. Beckett and Friend [6] solved the mixed convection flow between parallel vertical walls numerically at higher Rayleigh number. Joshi and Gebhart [15] solved the mixed convection in porous media adjacent to a vertical surface with uniform heat flux at the surface. Parang and Keyhani [24] studied the fully developed buoyancy-assisted mixed convection in a vertical annulus by using the Brinkman-extended Darcy model. Ramachandran *et al.* [26] investigated numerically laminar mixed convection in the two-dimensional stagnation flows around heated surfaces for both cases of an arbitrary wall temperature and arbitrary surface heat flux variations. Oosthuizen [23] investigated numerically the two-dimensional mixed convection flow over a horizontal plate in a saturated porous medium mounted near an impervious adiabatic horizontal surface and subject to a horizontal forced flow. Hadim and Chen [11] investigated the effect of Darcy number on the buoyancy-assisted mixed convection in the entrance region of a vertical channel with asymmetric heating at fixed values of the Reynolds number, Forchheimer number, Prandtl number and modified Grashof number.

The significance of suction/injection on the boundary layer control in the field of aerodynamics and space science is well recognized (Singh, [29]). Suction or injection of a fluid through the bounding surface as for example in mass transfer cooling, can significantly change the flow field and, as a consequence, affect the heat transfer rate from the plate (Ishak *et al.* [13]). In general, suction tends to increase the skin friction and heat transfer coefficient whereas injection acts in the opposite manner (Al-Sanea, [2]). This is well explored by Shojaefard *et al.* [28] where suction and injection were used to control fluid flow on the surface of subsonic aircraft. By controlling the flow as such, fuel consumption might be decreased by 30%, a considerable reduction in pollutant emission is achieved, and operating costs of commercial airplanes are reduced by at least 8% (Braslow, [5]).

Jha and Ajibade [14] investigated the free convective flow of heat generating/absorbing fluid between vertical parallel porous plates due to periodic heating of the porous plates. The analysis was performed by considering fully developed flow and steady-periodic regime.

In view of the amount of works done on the laminar flow in a saturated porous media with suction/injection, it becomes interesting to investigate the combined effects of the isothermal and isoflux heating conditions on the channel's walls.

II. Mathematical Analysis

We present the fully developed incompressible viscous laminar flow between two horizontal walls filled with a fluid saturated porous medium. The walls are separated by a distance a apart. We consider a coupled momentum and heat transfer by laminar flow for the steady state hydro-dynamically and thermally developed situations which have unidirectional flow of a viscous combustible reacting fluid in the x-direction between permeable boundaries at $\bar{y} = 0$ and $\bar{y} = a$ as in figure 1. It is assumed that on one wall ($\bar{y} = 0$), fluid is injected into the channel with certain constant velocity (v_0) and that it is sucked off from the other plate ($\bar{y} = a$) at the same rate. The channel is composed of a lower heated wall with surface constant temperature (isothermal) or constant heat flux (isoflux) while the upper wall is fixed and isothermal. We follow closely and modify the

models presented in Lamidi et al,[16] with additional term of Arrhenius heat reaction. As a result of these assumptions, the dimensional equations of continuity, motion and energy are obtained as follows

$$\frac{d\bar{v}}{d\bar{y}} = 0 \tag{1}$$

$$\rho V_0 \frac{d\bar{u}}{d\bar{y}} = \mu_e \frac{d^2 \bar{u}}{d\bar{y}^2} - \frac{\mu}{K} \bar{u} + G \tag{2}$$

$$\rho c_p V_0 \frac{dT}{d\bar{y}} = k \frac{d^2 T}{d\bar{y}^2} + \mu \left(\frac{d\bar{u}}{d\bar{y}} \right)^2 + QA_0^n e^{-\frac{E}{RT}} \tag{3}$$

Subjected to the boundary conditions

$$\bar{u} = 0, \quad T = T_a \quad \text{or} \quad \frac{dT}{d\bar{y}} = -\frac{q}{k} \quad \text{at} \quad \bar{y} = 0 \tag{4}$$

$$\bar{u} = 0, \quad T = T_a \quad \text{at} \quad \bar{y} = a, \quad 0 \leq \bar{y} \leq a \tag{5}$$

Introducing the dimensionless quantities

$$y = \frac{\bar{y}}{a}, \quad u = \frac{\mu \bar{u}}{Ga^2}, \quad M = \frac{\mu_e}{\mu}, \quad Da = \frac{K}{a^2}, \quad Pe = \frac{\rho c_p V_0 a}{k}, \quad Re = \frac{\rho V_0 a}{\mu}$$

$$Br = \frac{G^2 a^4}{\mu k \varepsilon T_0}, \quad \theta = \frac{E}{RT_0} (T - T_0), \quad \beta = \frac{a^2 QA_0^n e^{-\frac{E}{RT_0}}}{k \varepsilon T_0}, \quad \varepsilon = \frac{RT_0}{E} \tag{6}$$

where the variable parameters Br is the Brinkman number, Da is the Darcy number, Re is the suction/injection Reynolds number, Pe is the Peclet number, M is the ratio of effective viscosity of porous region to fluid. The equation of continuity in (1), on integration, gives $\bar{v} = \text{constant} = v_0$ (say) is the normal velocity of suction or injection at the walls accordingly as $v_0 > 0$ and $v_0 < 0$ respectively and $v_0 = 0$ represents the case of impermeable walls. The channel's walls are uniformly porous.

The physical quantities used in the expression (6) are defined in the nomenclature.

The equations (2) and (3) in dimensionless forms are obtained as follows

$$M \frac{d^2 u}{dy^2} - Re \frac{du}{dy} - \frac{u}{Da} = -1 \tag{7}$$

$$\frac{d^2 \theta}{dy^2} - Pe \frac{d\theta}{dy} + Br \left(\frac{du}{dy} \right)^2 + \beta e^{1+\theta} = 0 \tag{8}$$

Similarly, we non-dimensionalised the boundary conditions (4) and (5) to get

$$u = 0, \quad \theta = 0 \quad \text{or} \quad \frac{d\theta}{dy} = -1 \quad \text{at} \quad y = 0 \tag{9}$$

$$u = 0, \quad \theta = 0 \quad \text{at} \quad y = \lambda, \quad 0 \leq \lambda \leq 1 \tag{10}$$

In order to unify the isothermal heating and isoflux heating at one condition, we may write

$$\theta = 0 \quad \text{or} \quad \frac{d\theta}{dy} = -1 \quad \text{to} \quad A \frac{d\theta}{dy} + B\theta = C \quad \text{at} \quad y = 0 \quad \text{and} \quad \theta = 0 \quad \text{at} \quad y = \lambda \tag{11}$$

where A , B and C are constants depending on the isothermal heating or isoflux heating.

For the isothermal heating: $A=0$, $B=1$ and $C=0$

while for isoflux heating: $A=1$, $B=0$ and $C=-1$

Here we revisit equations (7) and (8) with $Re \neq 0$, $Pe \neq 0$ for imposition of wall suction/injection and $\beta \neq 0$ for a reacting flow, and the analytical solution for (8) is obtained for the temperature fields using an approximation (Ayeni, [3])

$$e^{(1+\theta)} \approx 1 + (e-2)\theta + \theta^2$$

hence(8) becomes

$$\frac{d^2 \theta}{dy^2} - Pe \frac{d\theta}{dy} + Br \left(\frac{du}{dy} \right)^2 = -\beta (1 + (e-2)\theta + \theta^2) \tag{12}$$

with the boundary conditions (9) and (10).

Equations (7) and (12) are second order differential equations with constant coefficients. The solution of (7), using the boundary conditions in (9) and (10) with the method of undetermined coefficients, could be easily obtained as

$$u(y) = a_1 e^{r_1 y} + a_2 e^{r_2 y} + Da, \tag{13}$$

Now using (13) in (12) we have

$$\frac{d^2 \theta}{dy^2} - Pe \frac{d\theta}{dy} + Br (r_1 a_1 e^{r_1 y} + r_2 a_2 e^{r_2 y})^2 = -\beta(1 + (e - 2)\theta + \theta^2) \tag{14}$$

Here, it is convenient to form a power series expansion in the Frank-Kamenetskii parameter β , i.e.

$$\theta = \sum_{i=0}^{\infty} \theta_i \beta^i \tag{15}$$

Now putting (15) in (14) and expanding asymptotically using the following asymptotic variable

$$\theta = \theta_0 + \beta \theta_1 + \beta^2 \theta_2^2 + \dots \tag{16}$$

and equating the powers of β to get the following sets of system of equations

$$\beta^0: \frac{d^2 \theta_0}{dy^2} - Pe \frac{d\theta_0}{dy} = -Br (r_1 a_1 e^{r_1 y} + r_2 a_2 e^{r_2 y})^2 \tag{17}$$

with the boundary conditions

$$A \frac{d\theta_0}{dy} + B \theta_0 = C \text{ at } y = 0 \text{ and } \theta_0 = 0 \text{ at } y = \lambda, \quad 0 \leq \lambda \leq 1 \tag{18}$$

and

$$\beta^1: \frac{d^2 \theta_1}{dy^2} - Pe \frac{d\theta_1}{dy} = -\beta(1 + (e - 2)\theta_0 + \theta_0^2) \tag{19}$$

with the boundary conditions

$$A \frac{d\theta_1}{dy} + B \theta_1 = C \text{ at } y = 0 \text{ and } \theta_1 = 0 \text{ at } y = \lambda, \quad 0 \leq \lambda \leq 1 \tag{20}$$

and

$$\beta^2: \frac{d^2 \theta_2}{dy^2} - Pe \frac{d\theta_2}{dy} = -\beta(1 + (e - 2)(\theta_0 + \theta_1) + 2\theta_0 \theta_1 + \theta_0^2) \tag{21}$$

with the boundary conditions

$$A \frac{d\theta_2}{dy} + B \theta_2 = C \text{ at } y = 0 \text{ and } \theta_2 = 0 \text{ at } y = \lambda, \quad 0 \leq \lambda \leq 1 \tag{22}$$

Now solving (17) using (18) the solution gives

$$\theta_0(y) = a_3 + a_4 a_5 e^{Pe y} - a_6 e^{2r_1 y} + (a_7 e^{y(r_1+r_2)} - a_8 e^{2r_2 y}) a_9 \tag{23}$$

Also solving (19) using (20), the solution gives

$$\theta_1(y) = (a_{20} a_{30} + a_{22} y + a_{31}) e^{Pe y} + a_{21} + a_{23} + a_{24} e^{2y(r_1+r_2)} - a_{25} (e^{r_1 y})^4 + a_{26} (e^{r_1 y})^2 - a_{27} e^{y(r_1+r_2)} + a_{28} e^{y(r_1+3r_2)} - a_{29} (e^{Pe y})^2 - a_{32} e^{y(Pe+r_1+r_2)} + a_{33} e^{y(Pe+2r_1)} - a_{34} (e^{r_2 y})^4 + a_{35} (e^{r_2 y})^2 + a_{36} e^{y(Pe+2r_2)} + a_{37} e^{y(3r_1+r_2)} \tag{24}$$

And finally solving (21) using (22) the solution gives

$$\begin{aligned} \theta_2(y) = & (a_{70} a_{92} + a_{93}) e^{Pe y} + a_{71} + a_{72} e^{2(2r_2+r_1)y} + a_{73} (e^{r_2 y})^4 + a_{74} (e^{r_2 y})^2 + (a_{75} - a_{97}) e^{(Pe+2r_2)y} + (a_{76} + a_{94}) \\ & e^{(Pe+r_1+r_2)y} + a_{77} e^{(Pe+4r_2)y} + a_{87} e^{(3r_1+r_2)y} + a_{90} e^{(Pe+2r_1)y} + a_{95} (e^{Pe y})^2 + a_{96} e^{(2Pe+r_1+r_2)y} + a_{99} e^{2(r_1+r_2)y} \\ & + a_{100} (e^{r_1 y})^4 + a_{101} e^{(Pe+3r_1+r_2)y} + a_{102} e^{2(Pe+2r_1)y} + a_{104} e^{(5r_1+r_2)y} + a_{106} e^{(Pe+4r_1)y} + a_{107} e^{2(2r_1+r_2)y} + a_{108} (e^{r_1 y})^2 \\ & + a_{109} e^{2(Pe+r_2)y} + a_{110} e^{(r_1+5r_2)y} + a_{111} e^{(r_1+r_2)y} - a_{112} (e^{r_2 y})^6 + y(a_{78} + a_{79}) e^{(Pe+2r_1)y} + a_{80} + a_{81} e^{(Pe+r_1+r_2)y} \\ & + a_{82} - a_{83} (e^{Pe y})^2 + a_{84} e^{(Pe+2r_2)y} + a_{85} e^{Pe y} + a_{86} + a_{88} e^{(Pe+2r_1+2r_2)y} + a_{89} e^{(r_1+3r_2)y} - a_{91} e^{(Pe+2r_1)y} \\ & + a_{103} e^{3(r_1+r_2)y} + a_{105} e^{(Pe+r_1+3r_2)y} + a_{113} (e^{Pe y})^3 - a_{114} (e^{r_1 y})^6 + a_{98} y^2 e^{Pe y} \end{aligned} \tag{25}$$

Now putting (23),(24) and (25) into (16) the general solution becomes

$$\begin{aligned}
 \theta(y) = & a_3 + a_4 a_5 e^{Pe y} - a_6 e^{2r_1 y} + (a_7 e^{y(r_1+r_2)} - a_8 e^{2r_2 y}) a_9 + \beta((a_{20} a_{30} + a_{22} y + a_{31}) e^{Pe y} + a_{21} + a_{23} \\
 & + a_{24} e^{2y(r_1+r_2)} - a_{25} (e^{r_1 y})^4 + a_{26} (e^{r_1 y})^2 - a_{27} e^{y(r_1+r_2)} + a_{28} e^{y(r_1+3r_2)} - a_{29} (e^{Pe y})^2 - a_{32} e^{y(Pe+r_1+r_2)} \\
 & + a_{33} e^{y(Pe+2r_1)} - a_{34} (e^{r_2 y})^4 + a_{35} (e^{r_2 y})^2 + a_{36} e^{y(Pe+2r_2)} + a_{37} e^{y(3r_1+r_2)}) + \beta^2((a_{70} a_{92} + a_{93}) e^{Pe y} + a_{71} \\
 & + a_{72} e^{2(2r_2+r_1)y} + a_{73} (e^{r_2 y})^4 + a_{74} (e^{r_2 y})^2 + (a_{75} - a_{97}) e^{(Pe+2r_2)y} + (a_{76} + a_{94}) e^{(Pe+r_1+r_2)y} + a_{77} e^{(Pe+4r_2)y} \\
 & + a_{87} e^{(3r_1+r_2)y} + a_{90} e^{(Pe+2r_1)y} + a_{95} (e^{Pe y})^2 + a_{96} e^{(2Pe+r_1+r_2)y} + a_{99} e^{2(r_1+r_2)y} + a_{100} (e^{r_1 y})^4 + a_{101} e^{(Pe+3r_1+r_2)y} \\
 & + a_{102} e^{2(Pe+2r_1)y} + a_{104} e^{(5r_1+r_2)y} + a_{106} e^{(Pe+4r_1)y} + a_{107} e^{2(2r_1+r_2)y} + a_{108} (e^{r_1 y})^2 + a_{109} e^{2(Pe+r_2)y} + a_{110} e^{(r_1+5r_2)y} \\
 & + a_{111} e^{(r_1+r_2)y} - a_{112} (e^{r_2 y})^6 + y(a_{78} + a_{79} e^{(Pe+2r_1)y} + a_{80} + a_{81} e^{(Pe+r_1+r_2)y} + a_{82} - a_{83} (e^{Pe y})^2 + a_{84} e^{(Pe+2r_2)y} \\
 & + a_{85} e^{Pe y} + a_{86}) + a_{88} e^{(Pe+2r_1+2r_2)y} + a_{89} e^{(r_1+3r_2)y} - a_{91} e^{(Pe+2r_1)y} + a_{103} e^{3(r_1+r_2)y} + a_{105} e^{(Pe+r_1+3r_2)y} \\
 & + a_{113} (e^{Pe y})^3 - a_{114} (e^{r_1 y})^6 + a_{98} y^2 e^{Pe y}), \tag{26}
 \end{aligned}$$

III. Results and Discussion

The dimensionless parameters governing the flow in the channel are suction/injection Reynolds, Re , Darcy number, Da , ratio of the effective viscosity of porous region to the viscosity of the fluid, M , Brinkman number, Br , Peclet number, Pe , and the Frank-Kamenetskii parameter, β , due to Arrhenius kinetic term. The outcome from the numerical computation is analysed in this section graphically with contour graphs for the case $Re \neq 0, Pe \neq 0$ (for imposition of suction/injection walls) and $\beta \neq 0$ (for a reacting flow) as against Lamidi et al. [16].

Figure 2 illustrates the dimensionless temperature distributions for different values of Frank-Kamenetskii parameter β , with other fluid flow parameters remain constant. It is noticed that an increase in the Frank-Kamenetskii parameter β due to the Arrhenius kinetics causes a further increase in the fluid temperature; this is due to combined effects of viscous dissipation and exothermic reaction. In addition, at one glance from this figure, it is deduced that the sharp decay in the fluid temperature near the wall suction as against the mild decay near the wall injection as β increases, this is due to the presence of suction/injection walls in the medium since the wall suction is to take away the warm solute on the wall thereby causing a reduction in the temperature of the fluid near the wall.

With isoflux case in figure 3, it was observed that the temperature is a decreasing function of β , however, the heat transfer is negative for all values of β for isoflux case in the presence of Arrhenius term. This implies that the heat transfer goes from the fluid to the wall.

In figure 4, the temperature of the fluid increases as Da increases in the channel with isothermal condition. The magnitude of the temperature is reduced further due to the reacting nature of the flow. A significant observation from this figure, also suggests that the enhancement of the fluid temperature near the wall suction as against the wall injection is due to the imposition of wall suction in the medium.

Figure 5 shows a contrary behavior of Da in isoflux case. It is noted that the temperature field decreases across the channel but remains constant along the channels as Da increases. This negates in totality, the usual trend in a non-reacting flow see Lamidi et al. [16]. This situation could be ascribed to the reacting nature of the flow which reveals that the presence of Frank-Kamenetskii parameter β suppresses the effect of Da in isoflux case.

Figure 6, for isothermal heating process, reveals that, the fluid temperature increases with a decrease in M . Also, due to the reacting nature of the fluid flow in the channel the parabolic nature of the flow was distorted and the magnitude of the temperature produced are very small as compared to that of Lamidi et al. [16] (non-reacting flow). Also the rate of decay of the temperature near the wall suction is very high.

Figure 7, in the case of isoflux heating process, however observes a steady situation of the temperature of the flow along the channel but decreases across the channel towards the wall suction as M increases as against the situations in figure 6 (isothermal case). This shows that the presence of the Frank-Kamenetskii parameter suppresses the influence of M as against its effects in Lamidi et al. [16] (non-reacting flow).

Figure 8 reflects the combined effects of Da and M on the temperature fields in isothermal case; it shows that the temperature increases with increase in Da and decrease in M when β is constant.

Figure 9 displays the combined effects of Da and M on the temperature field in isoflux case; with a cursory look, it reveals the hidden effects of both Da and M in figures 5 and 7 respectively, it shows that the temperature decreases with an increase in Da , and decrease in M .

Figure 10 is a plot of temperature fields against the dimensionless distance for different values of Peclet number, Pe . The said figure displays that the Peclet number, decreases the temperature at all points of the flow

fields with the usual trend of faster decay of the temperature near the suction wall as we also have in Amumeji [3] (non-reacting flow), however the profile is more distorted and smaller in magnitude in comparison to Amumeji [3] due to the reacting nature of the fluid. With the increase in Peclet number, the thermal conduction in the flow field is lowered and the viscosity of the flowing fluid becomes higher. In consequence, the molecular motion of the fluid elements is lowered down and therefore the flow field suffers a decrease in temperature as we increase Peclet number Pe .

In figure 11 with isoflux boundary conditions, we also note a contrary view to figure 10. We show that the fluid temperature is an increasing function of Peclet number, Pe along the channel, and a decreasing function across the channel. Furthermore, the temperature gradient is also observed to be exponentially higher near the outlet of the channel when Pe is higher. We also discover that the presence of wall suction retards the rate of increase in fluid temperature as Pe increases and decrease in temperature across the channel.

We present in figure 12 for isothermal heating process that, the fluid temperature increases with increase in Br . Also, due to the reacting nature of the fluid flow in the channel, the flow was slightly distorted and the fluid recorded lower temperatures in figure 12 compare to that of Amumeji [3] (non-reacting flow). Also the rate of enhancement near the suction wall is great, due to imposition of wall suction Reynolds number. This investigated the effect of viscous dissipation in the presence of suction/injection walls with isothermal process that the dimensionless temperature of a reacting fluid is higher near to the wall suction as Brinkman number increases. This combined effects of Br and M on the temperature profile can as well be easily confirmed in figure 14.

However, in the case of isoflux heating process, in figure 13, we observe a reverse situation where the fluid temperature increases as Br decreases and remains constant across the channel as against the situations in figure 12 (isothermal case). This effects could be easily noted in the simultaneous effects of Br and M on the temperature profile in figure 15. This shows that the presence of the Frank-Kamenetskii parameter suppresses the influence of Brinkman number Br as against its effects in Amumeji [3]. In this isoflux case, the temperature distributions are steadier across the channel towards the wall suction.

In figure 16 with isothermal condition, it is shown that the temperature of a reacting fluid increases with increase in wall injection Re . It is also seen that the temperature is well distributed throughout the channel but the temperature profile near the wall suction is more enhanced. It is also observed in the same figure that the temperature is known to increase faster if injection rate increases. The combined effect of injection Re and M is displayed in figure 18, where increase in injection Re and decrease in M increase the temperature distribution of the reacting flow.

In Figure 17 for isoflux case, it is observed that with increase in injection Re , the temperature remains constant along the channel up to a particular point near the channel outlet where there was a sudden sharp increase in the temperature very close to the wall injection. It is also noted that the temperature decreases across the channel. Figure 19, further reveals that the increase in both the injection Re and M increase the temperature of the reacting flow. This is also a deviation from the usual trend for M due to the reacting nature of the fluid flow in an isoflux case.

In figure 20, it is displayed that the fluid temperature decreases with increase in wall suction Re in isothermal case. It is further seen that there is a spontaneous decay in temperature field near the wall with suction. It is also observed in the same figure that the temperature is known to decrease faster if suction rate increases. The combined effects of suction Re and M is displayed in figure 22, where increase in both suction Re and M decrease the temperature distribution of the flow.

In an isoflux case in figures 21 and 23, an anomalous situation occurs where the temperature field increases as suction Reynolds number Re increases. This is the reverse of the usual trend and is attributed to the reacting nature of the flow. From figure 21, it is also observed that the temperature decreases across the channel towards the wall suction. Consequently, the parameter produces an inward flow of heating that accelerates the flux of heat to the wall suction.

IV. Conclusion

The theory of laminar flow in a channel filled with saturated porous media with isothermal and isoflux heating walls have been extensively studied. The various combinations of emerging parameters reveal much insight into the behaviours of the flow.

From our results, we established that:

- (i) increase in the Frank-Kamenetskii parameter β due to the Arrhenius kinetics causes a further increase in the fluid temperature in isothermal case whereas the temperature is a decreasing function of β in the case of isoflux.
- (ii) in isothermal case of a reacting flow, the temperature increases with increase in Da or Br or injection Re and decrease in Pe or M or suction Re .

- (iii) in isoflux case, the temperature of the reacting flow increases with increase in Pe or M or both suction/blowing Re and decrease in Br or Da , thereby creating reverse trends in the effects of Da , Br , M and suction Re in the presence of Arrhenius term.
- (iv) due to reacting nature of the fluid flow in the channel, the magnitude of the temperature produced, generally in the channel, are extremely small as compared to non-reacting flow.
- (v) the effect of some emerging parameters are suppressed in a reacting fluid flow due to the presence of the quadratic heating term.
- (vi) there is a scenario portraying the fluid temperature distributions of two heating processes at the boundary namely isothermal and isoflux, with the channel in the presence of wall suction/injection as well as reacting fluid flow.

Appendix

List of constants used to define the steady velocity and temperature

$$r_1 = \frac{1}{2M} \left(R_\epsilon + \sqrt{R_\epsilon^2 + \frac{4M}{Da}} \right), \quad r_2 = \frac{1}{2M} \left(R_\epsilon - \sqrt{R_\epsilon^2 + \frac{4M}{Da}} \right), \quad a_1 = -\frac{Da (e^{r_2 \lambda} - 1)}{e^{r_2 \lambda} - e^{r_1 \lambda}}, \quad a_2 = \frac{Da (e^{r_1 \lambda} - 1)}{e^{r_2 \lambda} - e^{r_1 \lambda}}$$

$$a_3 = (a_{15} e^{Pe \lambda} + a_{16} e^{2r_1 \lambda} + a_{17} a_9 e^{\lambda(r_1+r_2)} + a_{18} e^{2r_2 \lambda}) a_{19},$$

$$a_4 = \frac{(-4Pe + 4r_1 + 4r_2)(-\frac{1}{2}Pe + r_2)(-\frac{1}{2}Pe + r_1)}{Pe(-Pe + 2r_1)(-Pe + r_1 + r_2)(-Pe + 2r_2)}, \quad a_5 = (a_{10} - a_{11} e^{2r_1 \lambda} + a_{12} e^{\lambda(r_1+r_2)} - a_{13} e^{2r_2 \lambda}),$$

$$a_6 = \frac{(-4Pe + 4r_1 + 4r_2)(-\frac{1}{2}Pe + r_2)r_1 Bra_1^2}{(-Pe + 2r_1)(-Pe + r_1 + r_2)(-Pe + 2r_2)}, \quad a_7 = \frac{8a_1 a_2 r_1 r_2 Br (-\frac{1}{2}Pe + r_1)(-\frac{1}{2}Pe + r_2)}{r_1 + r_2},$$

$$a_8 = \frac{1}{4}(-4Pe + 4r_1 + 4r_2)(-\frac{1}{2}Pe + r_1) Bra_2^2 r_2, \quad a_9 = \frac{1}{(-Pe + 2r_1)(-Pe + r_1 + r_2)(-Pe + 2r_2)},$$

$$a_{10} = a_6(2Ar_1 + B) - a_7 a_9 (B + A(r_1 - r_2)) + a_8 a_9 (2Ar_2 + B) + C, \quad a_{11} = Ba_6,$$

$$a_{12} = Ba_7 a_9, \quad a_{13} = Ba_8 a_9, \quad a_{14} = \frac{1}{a_4(APe + B(1 - e^{Pe \lambda}))},$$

$$a_{15} = -C - a_6(2Ar_1 + B) + a_7 a_9 (B + A(r_1 + r_2)) - a_8 a_9 (2Ar_2 + B),$$

$$a_{16} = a_6(B + APe), \quad a_{17} = -a_7 a_9 (B + APe), \quad a_{18} = a_8 a_9 (B + APe), \quad a_{19} = \frac{1}{APe + B(1 - e^{Pe \lambda})},$$

$$a_{20} = (B(a_{24} e^{2(r_1+r_2)\lambda} - a_{25} (e^{r_1 \lambda})^4 + a_{26} (e^{r_2 \lambda})^2 - a_{27} e^{(r_1+r_2)\lambda} + a_{28} e^{(r_1+3r_2)\lambda} - a_{29} (e^{Pe \lambda})^2 - a_{32} e^{(Pe+r_1+r_2)\lambda} + a_{33} e^{(Pe+2r_1)\lambda} - a_{34} (e^{r_2 \lambda})^4 + a_{35} (e^{r_2 \lambda})^2 + a_{36} e^{(Pe+2r_2)\lambda} + a_{37} e^{(3r_1+r_2)\lambda}) + a_{38} + a_{39} e^{Pe \lambda}) a_{55},$$

$$a_{21} = -(a_{40} (e^{Pe \lambda})^2 + a_{41} e^{Pe \lambda} + a_{42} e^{3r_1 \lambda + r_2 \lambda} + a_{43} (e^{r_2 \lambda})^4 + a_{44} (e^{r_2 \lambda})^2 + a_{45} (e^{r_1 \lambda})^4 + a_{46} (e^{r_1 \lambda})^2 + a_{47} e^{2r_1 \lambda + 2r_2 \lambda} + a_{48} e^{Pe \lambda + 2r_1 \lambda} + a_{49} e^{Pe \lambda + r_1 \lambda + r_2 \lambda} + a_{50} e^{r_1 \lambda + 3r_2 \lambda} + a_{51} e^{r_1 \lambda + r_2 \lambda} + a_{52} e^{Pe \lambda + 2r_2 \lambda} + a_{53}) a_{54},$$

$$a_{22} = \frac{-\beta(2a_3 + (e-2))a_4 a_5}{Pe}, \quad a_{23} = \frac{\beta(2(e-2)a_3 + 1 + a_3^2)}{Pe}, \quad a_{24} = \frac{-\beta(2a_6 a_8 a_9 + a_7^2 a_9^2)}{(-Pe + 2r_1 + 2r_2)(2r_1 + 2r_2)},$$

$$a_{25} = \frac{1}{4} \frac{\beta a_6^2}{(-Pe + 4r_1)r_1}, \quad a_{26} = \frac{1}{2} \frac{\beta((e-2) + a_3)a_6}{(-Pe + 2r_1)r_1}, \quad a_{27} = \frac{((e-2) + 2a_3)\beta a_7 a_9}{(-Pe + r_1 + r_2)(r_1 + r_2)},$$

$$a_{28} = -\frac{2\beta a_7 a_8 a_9^2}{(-Pe + r_1 + 3r_2)(r_1 + 3r_2)}, \quad a_{29} = \frac{1}{2} \frac{\beta a_4^2 a_5^2}{Pe^2}, \quad a_{30} = \frac{1}{Pe}, \quad a_{31} = \frac{((e-2) + 2a_3)\beta a_4 a_5}{Pe^2},$$

$$a_{32} = \frac{2\beta a_4 a_5 a_7 a_9}{(Pe + r_1 + r_2)(r_1 + r_2)}, \quad a_{33} = \frac{\beta a_4 a_5 a_6}{r_1(Pe + 2r_2)}, \quad a_{34} = \frac{1}{4} \frac{\beta a_8^2 a_9^2}{r_2(-Pe + 4r_2)},$$

$$a_{35} = \frac{1}{2} \frac{\beta((e-2) + a_3)\beta a_8 a_9}{(-Pe + 2r_2)r_2}, \quad a_{36} = \frac{\beta a_4 a_5 a_8 a_9}{(Pe + 2r_2)r_2}, \quad a_{37} = \frac{2\beta a_6 a_7 a_9}{(-Pe + 3r_1 + r_2)(3r_1 + r_2)},$$

$$\begin{aligned}
 a_{38} &= C - A(a_{22} + 2a_{24}(r_2 + r_1) - 2(2a_{25} - a_{26})r_1 - a_{27}(r_2 + r_1) + a_{28}(r_1 + 3r_2) - (2a_{29} - a_{31})Pe \\
 &\quad - a_{32}(r_2 + r_1 + Pe) + a_{33}(Pe + 2r_1) - 2(2a_{34} - a_{35})r_2 + a_{36}(Pe + 2r_2) + a_{37}(3r_1 + r_2) \\
 &\quad - B(a_{24} - a_{25} + a_{26} - a_{27} + a_{28} - a_{29} + a_{31} - a_{32} + a_{33} - a_{34} + a_{35} + a_{36} + a_{37}), \\
 a_{39} &= B(a_{22}\lambda + a_{31}), \quad a_{40} = -(APe + B)a_{29}, \\
 a_{41} &= C - A(a_{22}(1 - \lambda Pe) + 2a_{24}(r_1 + r_2) - 2(2a_{25} - a_{26})r_1 - a_{27}(r_1 + r_2) + a_{28}(r_1 + 3r_2) - 2a_{29}Pe \\
 &\quad - a_{32}(r_2 + r_1 + Pe) + a_{33}(2r_1 + Pe) - 2(2a_{34} - a_{35})r_2 + a_{36}(Pe + 2r_2) + a_{37}(3r_1 + r_2) + Ba_{22}\lambda \\
 &\quad - Ba_{23} - Ba_{24} + Ba_{25} - Ba_{26} + Ba_{27} - Ba_{28} + Ba_{29} + Ba_{32} - Ba_{33} + Ba_{34} - Ba_{35} - Ba_{36} - Ba_{37}), \\
 a_{42} &= a_{37}(APe + B), \quad a_{43} = -a_{34}(APe + B), \quad a_{44} = a_{35}(APe + B), \quad a_{45} = -a_{25}(APe + B), \\
 a_{46} &= a_{26}(APe + B), \quad a_{47} = a_{24}(APe + B), \quad a_{48} = a_{33}(APe + B), \quad a_{49} = -a_{32}(APe + B), \\
 a_{50} &= a_{28}(APe + B), \quad a_{51} = -a_{27}(APe + B), \quad a_{52} = a_{36}(APe + B), \quad a_{53} = a_{23}(APe + B), \\
 a_{54} &= \frac{1}{APe + B(1 - e^{-Pe\lambda})}, \quad a_{55} = \frac{1}{a_{30}(APe + B(1 - e^{-Pe\lambda}))}, \quad a_{56} = -B(\lambda a_{85} + a_{93} + a_{98}\lambda^2), \\
 a_{57} &= B(a_{91} - \lambda a_{79}), \quad a_{58} = -B(\lambda a_{84} - a_{97}), \quad a_{59} = B(\lambda a_{83} - a_{95}), \\
 a_{60} &= A(2a_{72}(2r_2 + r_1) + 2(2a_{73} + a_{74})r_2 + a_{75}(Pe + 2r_2) + a_{76}(Pe + r_2 + r_1) + a_{77}(4r_2 + Pe) \\
 &\quad + (a_{78} + a_{79} + a_{80} + a_{81} + a_{82} - a_{83} + a_{84} + a_{85} + a_{86}) + a_{87}(3r_1 + r_2) + a_{88}(2r_1 + 2r_2 + Pe) \\
 &\quad + a_{89}(r_1 + 3r_2) + a_{90}(2r_1 + Pe) - a_{91}(2r_1 + Pe) + Pea_{93} + a_{94}(r_1 + r_2 + Pe) + 2a_{95}Pe \\
 &\quad + a_{96}(r_2 + r_1 + 2Pe) - a_{97}(Pe + 2r_2) + 2a_{99}(r_1 + r_2) + 4a_{100}r_1 + a_{101}(3r_1 + r_2 + Pe) \\
 &\quad + 2a_{102}(Pe + r_1) + 3a_{103}(r_2 + r_1) + a_{104}(r_2 + 5r_1) + a_{105}(3r_2 + r_1 + Pe) + a_{106}(4r_1 + Pe) \\
 &\quad + 2a_{107}(r_2 + 2r_1) + 2a_{108}r_1 + 2a_{109}(Pe + r_2) + a_{110}(r_1 + 5r_2) + a_{111}(r_1 + r_2) - 3a_{112}(2r_2 + Pe) \\
 &\quad - 6a_{114}r_1) + B(a_{72} + a_{73} + a_{74} + a_{75} + a_{76} + a_{77} - \lambda(a_{78} + a_{80} + a_{82} + a_{86}) + a_{87} + a_{88} \\
 &\quad + a_{89} + a_{90} - a_{91} + a_{93} + a_{94} + a_{95} + a_{96} - a_{97} + a_{99} + a_{100} + a_{101} + a_{102} + a_{103} + a_{104} + a_{105} \\
 &\quad + a_{106} + a_{107} + a_{108} + a_{109} + a_{110} + a_{111} - a_{112} + a_{113} - a_{114}) - C, \\
 a_{61} &= \frac{1}{a_{92}(APe + B(1 - e^{-Pe\lambda}))}, \quad a_{62} = \frac{1}{APe + B(1 - e^{-Pe\lambda})}, \quad a_{63} = -(B + APe)a_{62}a_{88}, \\
 a_{64} &= (B + APe)a_{62}a_{110}, \quad a_{65} = (B + APe)a_{62}a_{74}, \quad a_{66} = (B + APe)a_{62}a_{113}, \\
 a_{67} &= a_{62}(A(-2a_{72}(r_1 + 2r_2) - 2(2a_{73} + a_{74})r_2 - a_{75}(Pe + 2r_2) - a_{76}(Pe + r_1 + r_2) - a_{77}(4r_2 + Pe) - a_{78} - a_{79} \\
 &\quad - a_{80} - a_{81} - a_{82} + a_{83} - a_{84} - a_{85}(1 - \lambda Pe) - a_{86} - a_{87}(3r_1 + r_2) - a_{88}(Pe + 2r_1 + 2r_2) - a_{89}(r_1 + 3r_2) \\
 &\quad - a_{90}(2r_1 + Pe) + a_{91}(2r_1 + Pe) - a_{94}(Pe + r_1 + r_2) + a_{96}(r_1 + 2r_2 - 2Pe) + a_{97}(2r_2 + Pe) - 2a_{99}(r_1 + r_2) \\
 &\quad - 4a_{100}r_1 - a_{101}(Pe + r_2 + 3r_1) - 2a_{102}(r_1 + 2Pe) - a_{105}(3r_2 + r_1 + Pe) - a_{106}(Pe + 4r_1) - 2a_{107}(r_2 + 4r_1) \\
 &\quad - 2a_{109}(r_2 + Pe) + a_{110}(r_1 - 5r_2) - a_{111}(r_1 + r_2) - (3a_{103} + 2a_{108} - 6a_{114})r_1 - (a_{104} - 6a_{112})r_2 + (-2a_{95} \\
 &\quad + a_{98}\lambda^2 - 3a_{113})Pe) - 3a_{103}r_2 - 5a_{104}r_1) + C - B(a_{72} + a_{73} + a_{74} + a_{75} + a_{76} + a_{77} - \lambda a_{85} + a_{87} + a_{88} + a_{89} \\
 &\quad + a_{90} - a_{91} + a_{94} + a_{95} + a_{96} - a_{97} - a_{98}\lambda^2 - a_{99} + a_{100} + a_{101} + a_{102} + a_{103} + a_{104} + a_{105} + a_{106} + a_{107} + a_{108} \\
 &\quad + a_{109} + a_{110} + a_{111} - a_{112} + a_{113} - a_{114})), \\
 a_{68} &= (APe + B)a_{62}a_{102}, \quad a_{69} = (APe + B)a_{62}a_{99}, \\
 a_{70} &= -a_{61}(B(-a_{72}e^{2r_1\lambda + 4r_2\lambda} - a_{73}e^{(r_2\lambda)^4} - a_{74}e^{(r_2\lambda)^2} - a_{75}e^{Pe\lambda + 2r_2\lambda} - a_{77}e^{Pe\lambda + 4r_2\lambda} - \lambda a_{81}e^{\lambda(Pe + r_1 + r_2)} \\
 &\quad - a_{87}e^{3r_1\lambda + r_2\lambda} - a_{88}e^{Pe\lambda + 2r_1\lambda + 2r_2\lambda} - a_{89}e^{r_1\lambda + 3r_2\lambda} - a_{90}e^{Pe\lambda + 2r_1\lambda} - a_{94}e^{\lambda(Pe + r_1 + r_2)} - a_{96}e^{2Pe\lambda + r_1\lambda + r_2\lambda} \\
 &\quad - a_{99}e^{2(r_1\lambda + r_2\lambda)} - a_{100}(e^{(r_1\lambda)^4} + e^{(r_1\lambda)^6}) - a_{101}e^{Pe\lambda + 3r_1\lambda + r_2\lambda} - a_{102}e^{2(Pe\lambda + r_1\lambda)} - a_{103}e^{3(r_1\lambda + r_2\lambda)} \\
 &\quad - a_{104}e^{5r_1\lambda + r_2\lambda} - a_{105}e^{Pe\lambda + r_1\lambda + 3r_2\lambda} - a_{106}e^{Pe\lambda + 4r_1\lambda} - a_{107}e^{4r_1\lambda + 2r_2\lambda} - a_{108}e^{(r_1\lambda)^2} - a_{109}e^{2(Pe\lambda + r_2\lambda)} \\
 &\quad - a_{110}e^{r_1\lambda + 5r_2\lambda} - a_{111}e^{r_1\lambda + r_2\lambda} + a_{112}e^{(r_2\lambda)^6} - 2a_{113}e^{(Pe\lambda)^3} + a_{114}e^{(r_1\lambda)^6}) + a_{56}e^{Pe\lambda} + a_{58}e^{\lambda(Pe + 2r_2)} \\
 &\quad + a_{57}e^{\lambda(Pe + 2r_1)} + a_{59}(e^{Pe\lambda})^2 + a_{60} - a_{76}e^{Pe\lambda + r_1\lambda + r_2\lambda}),
 \end{aligned}$$

$$\begin{aligned}
 a_{71} &= a_{63} e^{\lambda(Pe+2r_1+2r_2)} - a_{64} e^{\lambda(r_1+5r_2)} - a_{65} (e^{r_2\lambda})^2 - a_{66} (e^{Pe\lambda})^3 - a_{67} e^{Pe\lambda} - a_{68} e^{2(Pe\lambda+2r_1\lambda)} - a_{69} e^{2r_1\lambda+2r_2\lambda} \\
 &- a_{115} e^{3(r_1\lambda+r_2\lambda)} - a_{116} e^{Pe\lambda+4r_1\lambda} - a_{117} (e^{Pe\lambda})^2 - a_{118} e^{r_1\lambda+r_2\lambda} - a_{119} e^{Pe\lambda+4r_2\lambda} - a_{120} e^{\lambda(Pe+r_1+r_2)} \\
 &- a_{121} (e^{r_2\lambda})^4 - a_{122} e^{Pe\lambda+3r_1\lambda+r_2\lambda} - a_{123} e^{2Pe\lambda+r_1\lambda+r_2\lambda} - a_{124} e^{5r_1\lambda+r_2\lambda} - a_{125} (e^{r_1\lambda})^4 - a_{126} e^{Pe\lambda+r_1\lambda+3r_2\lambda} \\
 &- a_{127} (e^{r_1\lambda})^6 - a_{128} e^{Pe\lambda+2r_2\lambda} - a_{129} e^{\lambda(Pe+2r_1)} - a_{130} e^{2Pe\lambda+2r_2\lambda} - a_{131} e^{\lambda(Pe+r_2)} - a_{132} e^{Pe\lambda+r_1\lambda+r_2\lambda} \\
 &- a_{133} e^{\lambda(3r_1+r_2)} - a_{134} e^{4r_1\lambda+2r_2\lambda} - a_{135} e^{4r_2\lambda+2r_1\lambda} - a_{136} e^{Pe\lambda+2r_1\lambda} - a_{137} - a_{138} (e^{r_2\lambda})^6 - a_{139} (e^{r_1\lambda})^2 \\
 &- a_{140} e^{r_1\lambda+3r_2\lambda}, \\
 a_{72} &= -\frac{2\beta a_7 a_9 a_{28}}{(-Pe+4r_2+2r_1)(4r_2+2r_1)} - \frac{2\beta a_6 a_{34}}{(-Pe+4r_2+2r_1)(4r_2+2r_1)} + \frac{2\beta a_8 a_9 a_{24}}{(-Pe+4r_2+2r_1)(4r_2+2r_1)}, \\
 a_{73} &= \frac{1}{4} \frac{2\beta a_3 a_{34} + \beta a_{34}(e-2)}{(-Pe+4r_2)r_2} + \frac{2\beta a_8 a_9 a_{24}}{(-Pe+4r_2+2r_1)(4r_2+2r_1)}, \\
 a_{74} &= \beta \left(\frac{a_8 a_9 a_{21} + a_8 a_9 a_{23} - a_3 a_{35} + a_3 a_8 a_9}{(-Pe+2r_2)r_2} + \frac{1}{2} \frac{(a_8 a_9 - a_{35})(e-2)}{(-Pe+2r_2)r_2} \right), \\
 a_{75} &= \beta \left(\frac{-a_3 a_{36} + a_8 a_9 a_{31} - a_4 a_5 a_{35} + a_4 a_5 a_8 a_9 + a_8 a_9 a_{20} a_{30}}{(-Pe+2r_2)r_2} - \frac{1}{2} \frac{a_{36}(e-2) - a_8 a_9 a_{22}}{(-Pe+2r_2)r_2} \right) \\
 a_{76} &= \frac{2\beta}{(r_1+r_2)(Pe+r_1+r_2)} \left(\frac{a_7 a_9 a_{22}}{(r_1+r_2)} + a_4 a_5 a_{27} + a_3 a_{32} - a_7 a_9 a_{20} a_{30} - a_7 a_9 a_{31} - a_4 a_5 a_7 a_9 + \frac{1}{2} a_{32}(e-2) \right) \\
 a_{77} &= \frac{1}{2} \beta \left(\frac{a_8 a_9 a_{36} + a_4 a_5 a_{34}}{(Pe+4r_2)r_2} \right), \quad a_{78} = \frac{\beta a_{21}(e-2)}{Pe}, \quad a_{79} = \frac{\beta a_6 a_{22}}{r_1(Pe+2r_1)}, \quad a_{80} = \frac{\beta a_3^2}{Pe}, \\
 a_{81} &= \frac{2\beta a_7 a_9 a_{22}(r_1-r_2)}{(Pe+r_1+r_2)(r_1+r_2)^2}, \quad a_{82} = \frac{\beta((e-2)(a_3+a_{23})+1)}{Pe}, \quad a_{83} = \frac{\beta a_4 a_5 a_{22}}{Pe^2}, \\
 a_{84} &= \frac{\beta a_8 a_9 a_{22}}{r_2(Pe+2r_2)}, \\
 a_{85} &= \frac{\beta}{Pe} ((e-2)(-a_4 a_5 - a_{20} a_{30} + \frac{1}{Pe} a_{22} - a_{31}) - 2a_3 a_{20} a_{30} - 2a_4 a_5 a_{23} - 2a_3 a_{31} + \frac{2}{Pe} a_3 a_{22} - a_4 a_5 a_{21} - a_3 a_4 a_5) \\
 a_{86} &= \frac{2\beta a_3(a_{21}+a_{23})}{Pe}, \quad a_{87} = 2\beta \left(\frac{-a_7 a_9 a_{26} - a_6 a_{27} - a_3 a_{37} + a_6 a_7 a_9 - a_{37}(e-2)}{(-Pe+r_1+r_2)(3r_1+r_2)} \right), \\
 a_{88} &= 2\beta \left(\frac{a_4 a_5 a_{24} - a_8 a_9 a_{33} - a_6 a_{36} + a_7 a_9 a_{32}}{(Pe+2r_1+2r_2)(2r_1+2r_2)} \right), \quad a_{89} = 2\beta \left(\frac{a_7 a_8 a_9^2 - a_3 a_{28} - a_8 a_9 a_{27} + a_7 a_9 a_{35} - \frac{1}{2} a_{28}(e-2)}{(-Pe+r_1+3r_2)(r_1+3r_2)} \right), \\
 a_{90} &= \beta \left(\frac{-a_3 a_{33} + a_4 a_5 a_6 - a_4 a_5 a_{26} + a_6 a_{31} - \frac{1}{2} a_{33}(e-2)}{(Pe+2r_1)r_1} - \frac{1}{2} \frac{a_6 a_{22}}{(Pe+2r_1)r_1^2} \right), \quad a_{91} = \frac{\beta a_6 a_{22}}{(Pe+2r_1)^2 r_1}, \quad a_{92} = \frac{1}{Pe}, \\
 a_{93} &= 2\beta \left(\frac{a_3 a_{31} - \frac{1}{Pe} a_3 a_{22} + a_3 a_4 a_5 + a_4 a_5 a_{23} + a_3 a_{20} a_{30} + a_4 a_5 a_{21}}{Pe^2} + \frac{1}{2} \frac{(a_4 a_5 + a_{20} a_{30} - \frac{1}{Pe} a_{22} + a_{31})(e-2)}{Pe^2} \right)
 \end{aligned}$$

$$a_{94} = \left(\frac{2\beta a_7 a_9 a_{22} (r_1 + r_2)}{(Pe + r_1 + r_2)^2 (r_1 + r_2)^2} \right), \quad a_{95} = \frac{\beta}{2Pe^2} \left(2a_3 a_{29} - a_4^2 a_5^2 + \frac{3}{Pe} a_4 a_5 a_{22} - 2a_4 a_3 a_{31} - 2a_4 a_5 a_{20} a_{30} + a_{29} (e - 2) \right)$$

$$a_{96} = 2\beta \left(\frac{a_4 a_5 a_{32} + a_7 a_9 a_{29}}{(Pe + r_1 + r_2)(2Pe + r_1 + r_2)} \right), \quad a_{97} = \frac{\beta a_8 a_9 a_{22}}{(Pe + 2r_2)^2 r_2}, \quad a_{98} = -\frac{1}{2}\beta \frac{a_{22} (e - 2) + 2a_3 a_{22}}{Pe},$$

$$a_{99} = \beta \left(-2 \frac{a_3 a_{24} + a_6 a_8 a_9 - a_6 a_{35} - a_7 a_9 a_{27} - a_8 a_9 a_{26}}{(-Pe + 2r_1 + 2r_2)(2r_1 + 2r_2)} - \frac{a_{24} (e - 2) + a_7^2 a_9^2}{(-Pe + 2r_1 + 2r_2)(2r_1 + 2r_2)} \right),$$

$$a_{100} = \beta \left(\frac{1}{2} \frac{a_3 a_{25} + a_6 a_{26}}{(-Pe + 4r_1)r_1} - \frac{1}{4} \frac{a_6^2 - a_{25} (e - 2)}{(-Pe + 4r_1)r_1} \right), \quad a_{101} = \beta \left(-2 \frac{a_4 a_5 a_{37} + a_6 a_{32} + a_7 a_9 a_{33}}{(3r_1 + r_2 + Pe)(3r_1 + r_2)} \right),$$

$$a_{102} = \beta \left(-2 \frac{a_4 a_5 a_{33} + a_6 a_{29}}{(2r_1 + Pe)(2Pe + 2r_1)} \right), \quad a_{103} = \beta \left(2 \frac{a_6 a_{28} - a_7 a_9 a_{24} + a_8 a_9 a_{37}}{(3r_1 + 3r_2 - Pe)(3r_1 + 3r_2)} \right),$$

$$a_{104} = \beta \left(2 \frac{a_6 a_{37} + a_7 a_9 a_{25}}{(5r_1 + r_2 - Pe)(5r_1 + r_2)} \right), \quad a_{105} = \beta \left(-2 \frac{a_4 a_5 a_{28} + a_7 a_9 a_{36} + a_8 a_9 a_{32}}{(r_1 + 3r_2 + Pe)(r_1 + 3r_2)} \right),$$

$$a_{106} = \beta \left(\frac{1}{2} \frac{a_4 a_5 a_{25} + a_6 a_{33}}{(4r_1 + Pe)r_1} \right), \quad a_{107} = \beta \left(2 \frac{a_6 a_{24} - a_7 a_9 a_{37} - a_8 a_9 a_{25}}{(4r_1 + 2r_2 - Pe)(4r_1 + 2r_2)} \right),$$

$$a_{108} = \beta \left(\frac{a_3 a_6 - a_3 a_{26} + a_6 a_{21} + a_6 a_{23}}{(2r_1 - Pe)r_1} - \frac{1}{2} \frac{(a_6 - a_{26})(e - 2)}{(2r_1 - Pe)r_1} \right), \quad a_{109} = -2\beta \left(\frac{a_4 a_5 a_{36} + a_8 a_9 a_{29}}{(2r_2 + Pe)(2r_2 + 2Pe)} \right),$$

$$a_{110} = 2\beta \frac{a_7 a_9 a_{34} + a_8 a_9 a_{28}}{(r_1 + 5r_2)(r_1 + 5r_2 - Pe)}, \quad a_{111} = \beta \left(\frac{-2(a_3 a_7 a_9 - a_3 a_{27} + a_7 a_9 a_{21} + a_7 a_9 a_{23}) - (a_7 a_9 - a_{27})(e - 2)}{(r_1 + r_2 - Pe)(r_1 + r_2)} \right),$$

$$a_{112} = \frac{\beta}{3} \frac{a_8 a_9 a_{34}}{r_2 (6r_2 - Pe)}, \quad a_{113} = \frac{\beta}{3} \frac{a_4 a_5 a_{29}}{Pe^2}, \quad a_{114} = \frac{\beta}{3} \frac{a_6 a_{25}}{r_1 (6r_1 - Pe)}, \quad a_{115} = a_{62} a_{103} (B + APe),$$

$$a_{116} = a_{62} a_{106} (B + APe), \quad a_{117} = a_{62} (-a_{83} \lambda + a_{95})(B + APe), \quad a_{118} = a_{62} a_{111} (B + APe),$$

$$a_{119} = a_{62} a_{77} (B + APe), \quad a_{120} = a_{62} (a_{81} \lambda + a_{94})(B + APe), \quad a_{121} = a_{62} a_{73} (B + APe),$$

$$a_{122} = a_{62} a_{101} (B + APe), \quad a_{123} = a_{62} a_{96} (B + APe), \quad a_{124} = a_{62} a_{104} (B + APe),$$

$$a_{125} = a_{62} a_{100} (B + APe), \quad a_{126} = a_{62} a_{105} (B + APe), \quad a_{127} = -a_{62} a_{114} (B + APe),$$

$$a_{128} = a_{62} a_{75} (B + APe), \quad a_{129} = a_{62} (a_{79} \lambda - a_{91})(B + APe), \quad a_{130} = a_{62} a_{109} (B + APe),$$

$$a_{131} = a_{62} (a_{84} \lambda - a_{97})(B + APe), \quad a_{132} = a_{62} a_{76} (B + APe), \quad a_{133} = a_{62} a_{87} (B + APe),$$

$$a_{134} = a_{62} a_{107} (B + APe), \quad a_{135} = a_{62} a_{72} (B + APe), \quad a_{136} = a_{62} a_{90} (B + APe),$$

$$a_{136} = a_{62} a_{90} (B + APe), \quad a_{137} = a_{62} \lambda (a_{78} + a_{80} + a_{82} + a_{86})(B + APe),$$

$$a_{138} = -a_{62} a_{112} (B + APe), \quad a_{139} = a_{62} a_{108} (B + APe), \quad a_{140} = a_{62} a_{89} (B + APe),$$

References

- [1]. A.K. Al-Hadrami, L. Elliot and D.B.Ingham, A New Model for Viscous Dissipation inPorous Media Across a Range of Permeability Values, *Transport Porous Media*, 53, 2003, 117-122.
- [2]. S.A. Al-Sanea, Mixed convection heat transfer along a continuously moving heated vertical plate with suction or injection, *Int. J. Heat Mass Transfer*, 47, 2004, 1445-1465.
- [3]. O.T. Amumeji, Analysis of a Non-Reacting Laminar Fluid Flow with Viscous Dissipation through a Porous Channel Formed by Two Parallel Horizontal Permeable Walls. *Journal of Natural Sciences Research*, 5(7), 2015, 7-20.
- [4]. R.O. Ayeni, On the explosion of chain thermal reactions, *Journal of Australian Mathematical Society*, 24, 1982, 194-202.

- [5]. A.L. Braslow, History of Suction-type Laminar Flow control with emphasis on Flight Research American Institute of Aeronautics and Astronautics, Washington D.C, 1999.
- [6]. [6] P.M. Beckett, and I.E. Friend, Combined natural and forced convection between parallel walls developing flow at higher Rayleigh numbers, *Int. J. Heat Mass Transfer*, 27, 1984, 611-621.
- [7]. P. Cheng, Similarity solution for mixed convection from horizontal impermeable surface in saturated porous medium, *Int. J. Heat Mass Transfer*, 20, 1977, 893-898.
- [8]. H. Darcy, *Les Fontaines Publiques de la Ville de Dijon* ('The Public Fountains of the Town of Dijon') Dalmont, (Paris, 1856).
- [9]. S.S. Dass, M. Mohanty, J.P. Panda, and S.K. Sahoo, Hydromagnetic Couette Flow and Heat Transfer, *Journal of Naval Architecture and Marine Engineering*. ANAME Publication, 2008.
- [10]. R.M. Fand, T.E. Steinberg, and P. Cheng, Natural convection heat transfer from a horizontal cylinder embedded in a porous medium, *Int. J. Heat Mass Transfer*, 29, 1986, 119-133.
- [11]. A. Hadi M, and A. Chen, Non-Darcy Mixed convection in a vertical porous channel, *J. Thermo Physics and Heat Transfer*, 8, 1994, 805-808.
- [12]. D.B. Ingham, and I. Pop, *Transport Phenomena in Porous Media*, (Pergamon Press, Oxford, 1998).
- [13]. A. Ishak, J.H. Merkin, R. Nazar, and I. Pop, Mixed convection boundary layer flow over a permeable vertical surface with prescribed wall heat flux, *ZAMP*, 59, 2008, 100-123.
- [14]. B.K. Jha, and A.O. Ajibade, free convective flow of heat generating/absorbing fluid between vertical Parallel porous plates with periodic heat input, *Int. Commun. Heat Mass Transfer*, 36, 2009, 624-631.
- [15]. Y. Joshi, and B. Gebhart, Mixed convection in porous media adjacent to a vertical uniform heat flux surface, *Int. J. Heat Mass Transfer*, 28, 1985, 1783-1786.
- [16]. O.T. Lamidi, and R.O. Ayeni, Analytical Solution of a Steady Non-Reacting Laminar Fluid Flow in a Channel Filled with Saturated Porous Media with Two Distinct Horizontal Impermeable Wall Conditions, *Journal of Natural Sciences Research*, 2(3), 2012, 80-90.
- [17]. G. Lauriat, and V. Prasad, Natural convection in a vertical porous cavity a numerical study for Brinkman extended Darcy formulation, *ASME HTD*, 56, 1986, 13-22.
- [18]. O.D. Makinde, Thermal Ignition in a Reactive Viscous Flow through a Channel Filled with a Porous Medium, *Journal of Heat Transfer by ASME*, 128, 2006, 601-604.
- [19]. O.D. Makinde, and E. Osalusi, Second Law Analysis of Laminar flow in a channel filled with saturated porous media, *Entropy ISSN 1099-4300*, 7(2), 2005, 148-160.
- [20]. B.S. Mazumder, Taylor diffusion for a natural convective flow through a vertical channel, *Int. J. Engineering Sciences*, 19, 1981, 771-779.
- [21]. A.K. Mishra, T. Paul, and A.K. Singh, Mixed convection in a porous medium bounded by two vertical walls, *Forschung im Ingenieurwesen, Springer Verlag*, 67, 2001, 198-205.
- [22]. D.A. Nield and A. Benja, *Convection in Porous Media*, (2nd ed, Springer, New York, 1999).
- [23]. P.H. Oosthuizen, Mixed convective heat transfer from a heated horizontal plate in a porous medium near an impermeable surface, *ASME, J. Heat Transfer*, 110, 1988, 390-394.
- [24]. M. Parang, and M. Keyhani, Boundary effects in laminar mixed convection flow through an annular porous medium, *ASME J. Heat Transfer*, 109, 1987, 1039-1041.
- [25]. T. Paul, B.K. Jha, and A.K. Singh, Transient Free Convective Flow in a Channel with Constant Heat Flux on Walls, *Heat and Mass Transfer*, 32, 1996, 61-63.
- [26]. N. Ramachandran, T.S. Chen, and B.F. Armaly, Mixed convection in stagnation flows adjacent to vertical surfaces, *ASME, J. Heat Transfer*, 110, 1988, 373-377.
- [27]. P. Ranganathan, and R. Viskanta, Mixed Convection Boundary layer flow along a vertical surface in a porous medium, *Heat Transfer*, 7, 1984, 305-317.
- [28]. M.H. Shojaefard, A.R. Noorpoor, A. Avanesians and M. Ghaffapour, Numerical Investigation of Flow Control by Suction and Injection on a Subsonic Airfoil, *American Journal of Applied Sciences*, 20(10), 2005, 1474-1480.
- [29]. A.K. Singh, Stokes Problem for a Porous Vertical Plate with heat Sinks by Finite Difference Method, *Astrophysics and Space Science*, 103, 1984, 241-248.
- [30]. T.W. Tong, and E. Subramaniam, A boundary layer analysis for natural convection in vertical porous enclosures, use of the Brinkman-extended Darcy model, *Int. Journal on Heat Mass Transfer*, 28(3), 1985, 563-571.
- [31]. V. Vafai, and C.L. Tien, Boundary and inertia effects on flow and heat transfer in porous media, *Int. Jr. Heat and Mass Transfer*, 24, 1981, 195-204.
- [32]. P.D. Varmal and D.S. Chauhan, Unsteady flow of a Viscous incompressible fluid through a circular naturally permeable tube surrounded by a porous material, *Indian Jr. of Tech.*, 24, 1986, 63-65.

Figures

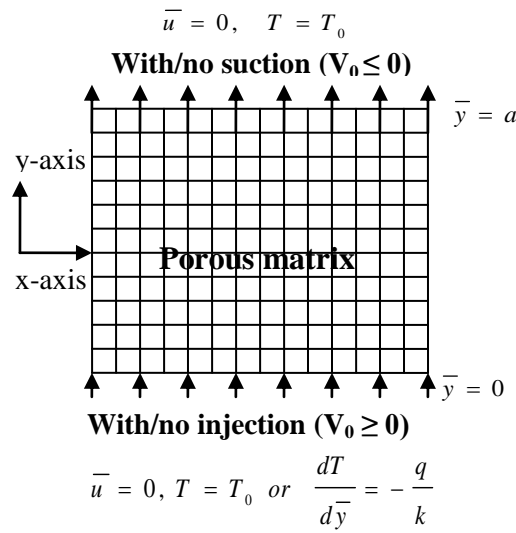


Figure 1: Problem Geometry

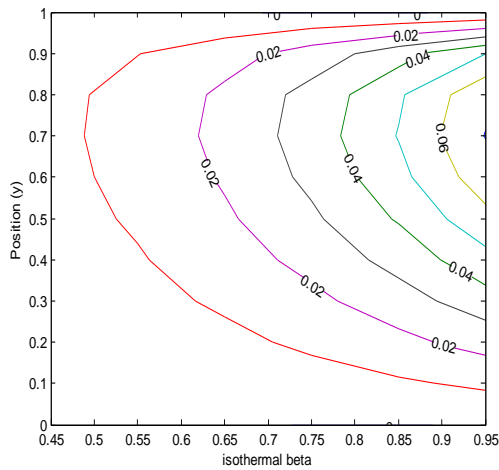


Figure 2: Contour graph of temperature $\theta(y)$ at various values of β with $Da = 0.1$
 $Re = 5.0, Br = 0.3, Pe = 7.1, M = 1.0$
 (isothermal) for equation (25)

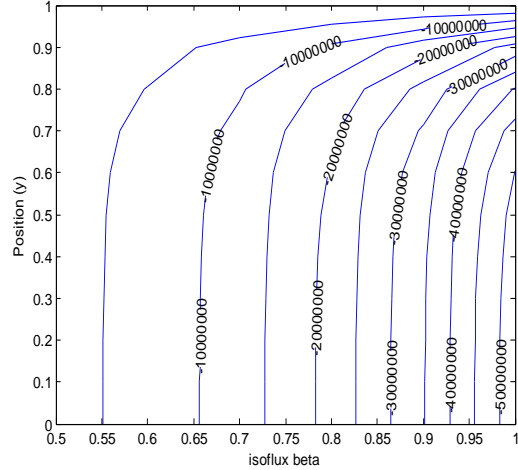


Figure 3: Contour graph of temperature $\theta(y)$ at various values of β with $Da = 0.1$
 $Re = 5.0, Br = 0.3, Pe = 7.1, M = 1.0$
 (isoflux) for equation (25)

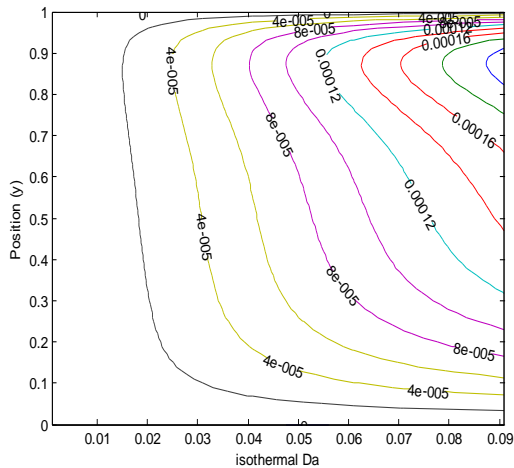


Figure 4: Contour graph of temperature $\theta(y)$ at various values of Da with $\beta = 0.04$

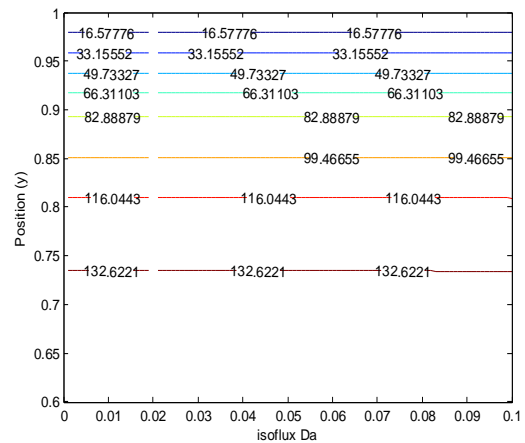


Figure 5: Contour graph of temperature $\theta(y)$ at various values of Da with $\beta = 0.04$

Re = 5.0, Br = 0.3, Pe = 7.1, M = 1.0
(isothermal) for equation (25)

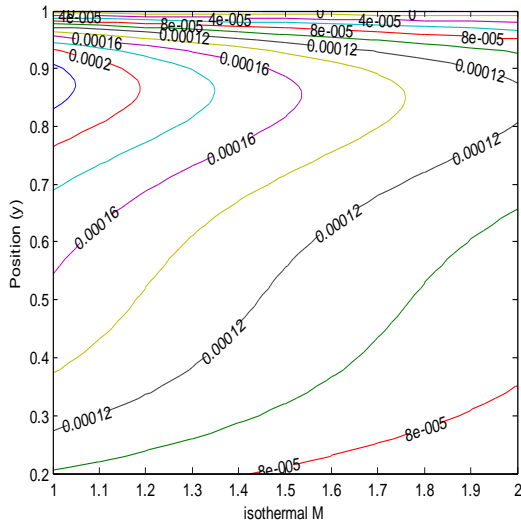


Figure 6: Contour graph of temperature $\theta(y)$ at various values of M with $\beta = 0.04$
Re = 5.0, Br = 0.3, Pe = 7.1, Da = 0.1
(isothermal) for equation (25)

Re = 5.0, Br = 0.3, Pe = 7.1, M = 1.0
(isoflux) for equation (25)

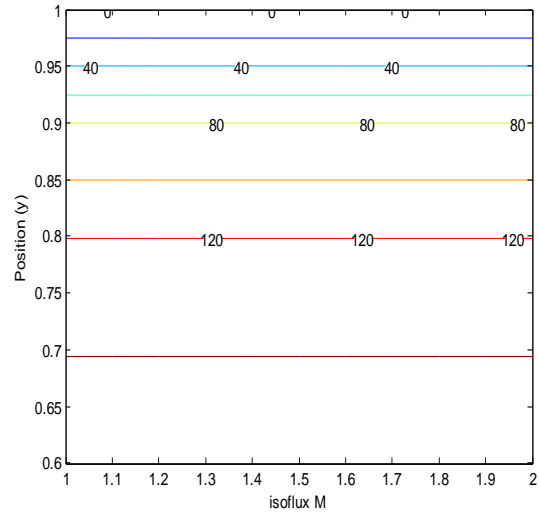


Figure 7: Contour graph of temperature $\theta(y)$ at various values of M with $\beta = 0.04$
Re = 5.0, Br = 0.3, Pe = 7.1, Da = 0.1
(isoflux) for equation (25)

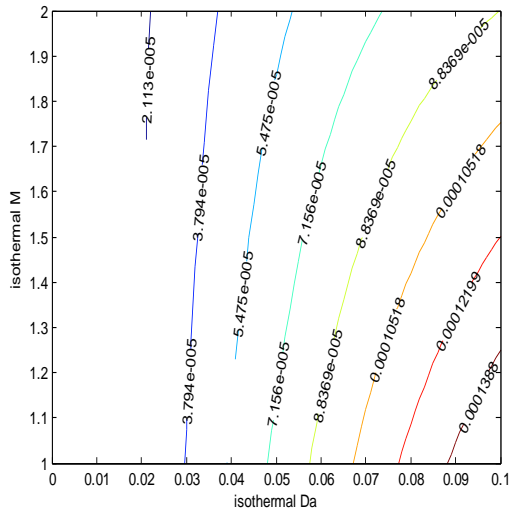


Figure 8: Contour graph of temperature $\theta(y)$ at various values of Da and M with $\beta = 0.04$, Re = 5.0, Br = 0.3, Pe = 7.1, y = 0.5, (isothermal) for equation (25)

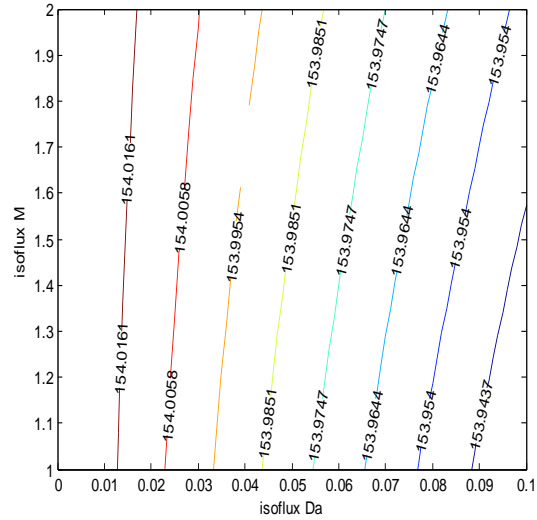


Figure 9: Contour graph of temperature $\theta(y)$ at various values of Da and M with $\beta = 0.04$, Re = 5.0, Br = 0.3, Pe = 7.1, y = 0.5, (isoflux) for equation (25)

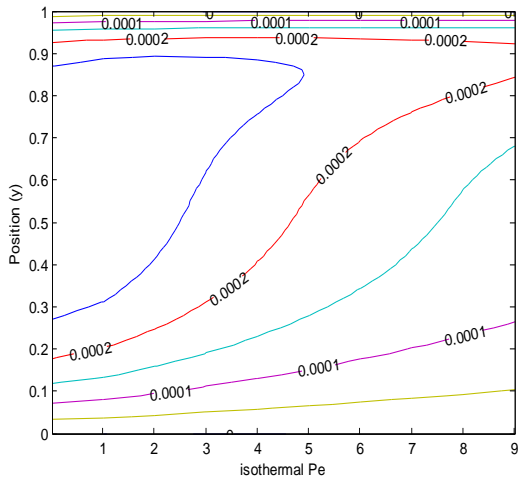


Figure 10: Contour graph of temperature $\theta(y)$ at various values of Pe with $\beta = 0.04$
 Re = 5.0, Br = 0.3, M = 1.0, Da = 0.1
 (isothermal) for equation (25)

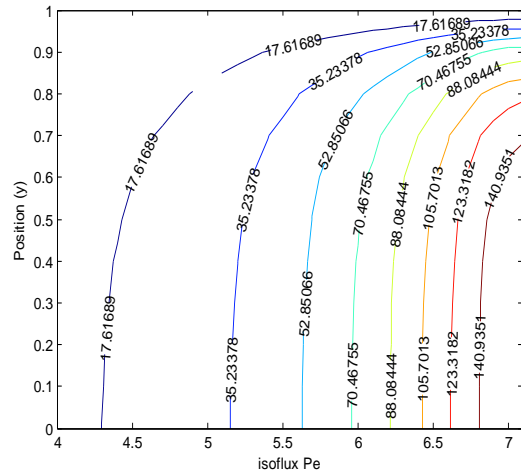


Figure 11: Contour graph of temperature $\theta(y)$ at various values of Pe with $\beta = 0.04$
 Re = 5.0, Br = 0.3, M = 1.0, Da = 0.1
 (isoflux) for equation (25)

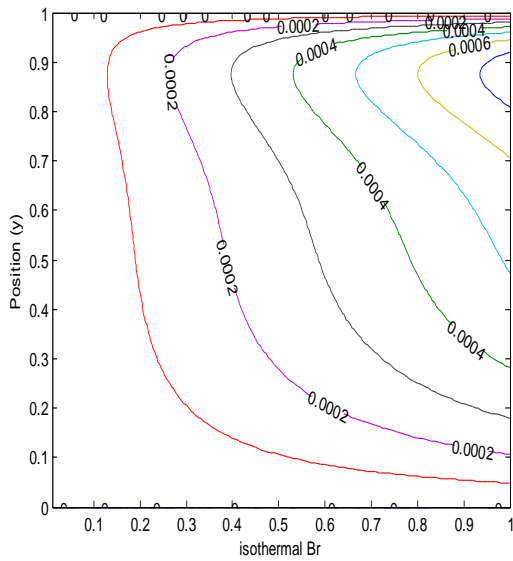


Figure 12: Contour graph of temperature $\theta(y)$ at various values of Br with $\beta = 0.04$
 Re = 5.0, Br = 0.3, Pe = 7.1, Da = 0.1
 (isothermal) for equation (25)

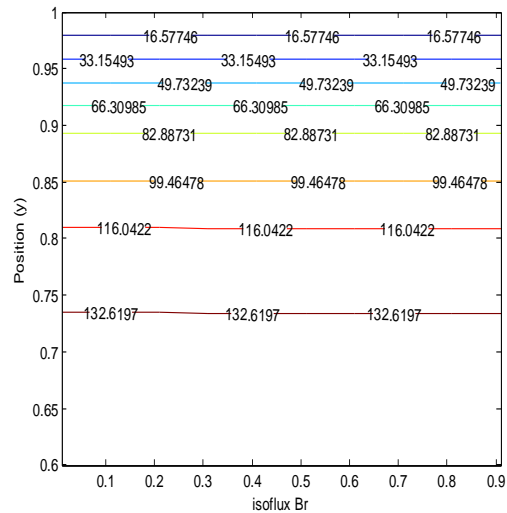


Figure 13: Contour graph of temperature $\theta(y)$ at various values of Br with $\beta = 0.04$
 Re = 5.0, Br = 0.3, Pe = 7.1, Da = 0.1
 (isoflux) for equation (25)

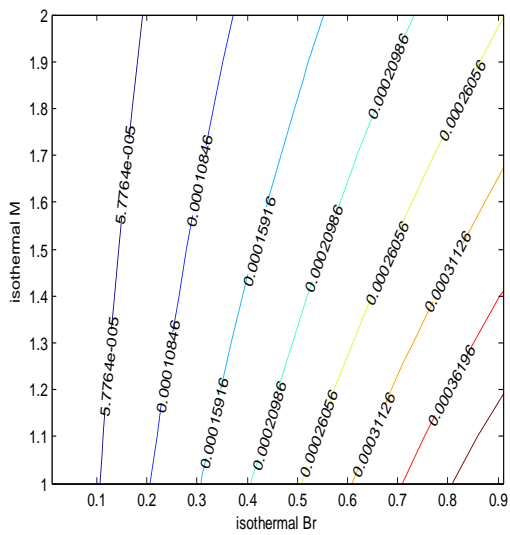


Figure 14: Contour graph of temperature $\theta(y)$ at various values of Br and M with $\beta = 0.04$, $Re = 5.0$, $Da = 0.1$, $Pe = 7.1$, $y = 0.5$, (isothermal) for equation (25)

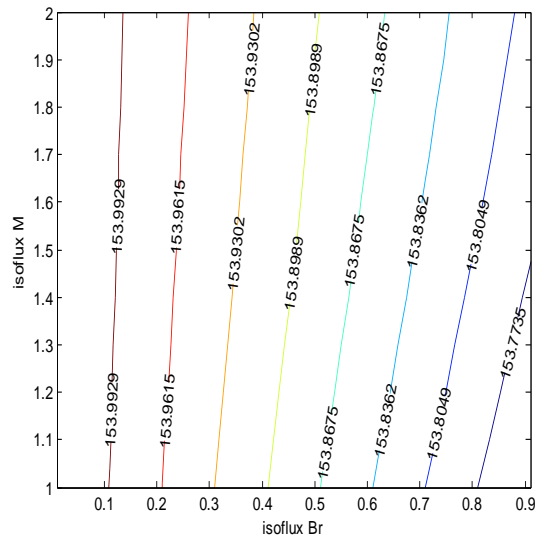


Figure 15: Contour graph of temperature $\theta(y)$ at various values of Br and M with $\beta = 0.04$, $Re = 5.0$, $Da = 0.1$, $Pe = 7.1$, $y = 0.5$, (isoflux) for equation (25)

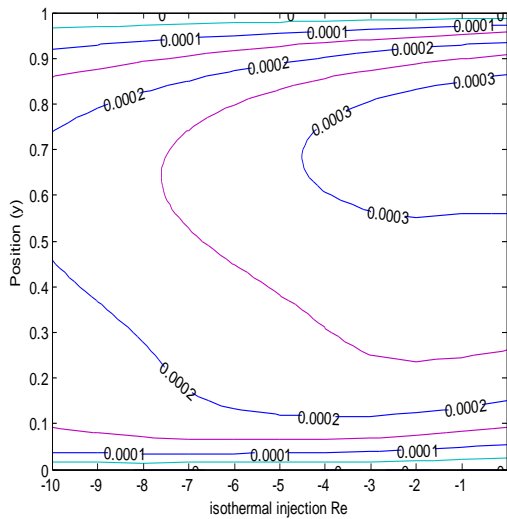


Figure 16: Contour graph of temperature $\theta(y)$ at various values of injection Re with $\beta = 0.04$, $M = 1.0$, $Br = 0.3$, $Pe = 7.1$, $Da = 0.1$ (isothermal) for equation (25)

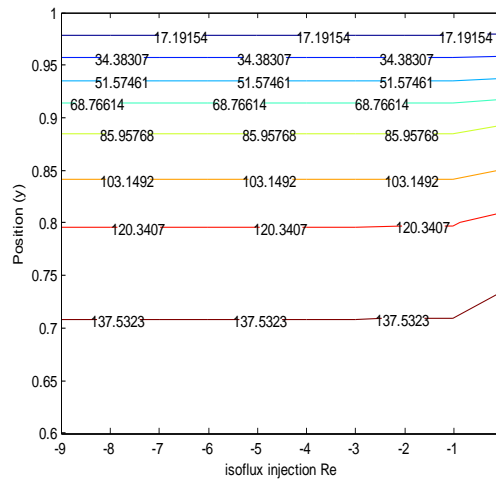


Figure 17: Contour graph of temperature $\theta(y)$ at various values of injection Re with $\beta = 0.04$, $M = 1.0$, $Br = 0.3$, $Pe = 7.1$, $Da = 0.1$ (isoflux) for equation (25)

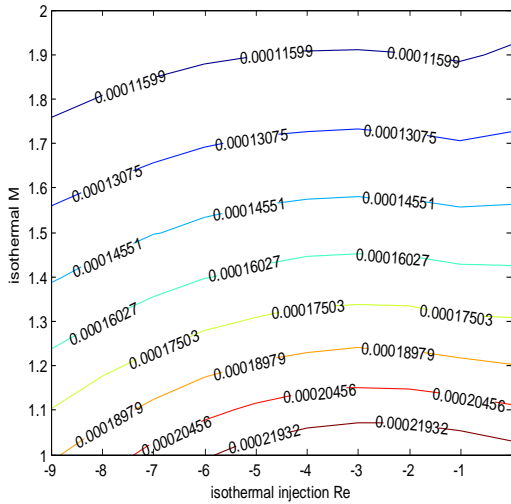


Figure 18: Contour graph of temperature $\theta(y)$ at various values of injection Re and M with $\beta = 0.04$, $Br = 0.3$, $Pe = 7.1$, $Da = 0.1$ (isothermal) for equation (25)

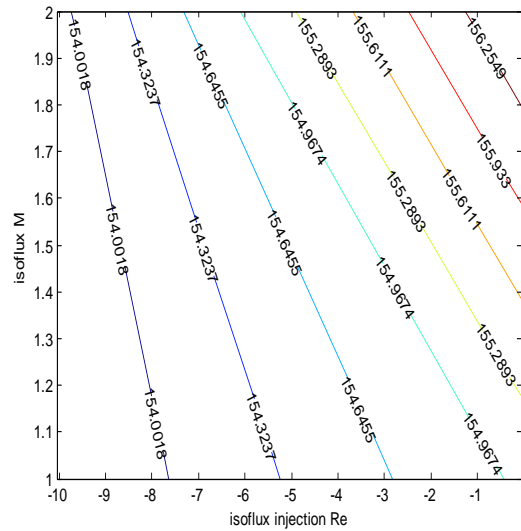


Figure 19: Contour graph of temperature $\theta(y)$ at various values of injection Re and M with $\beta = 0.04$, $Br = 0.3$, $Pe = 7.1$, $Da = 0.1$ (isoflux) for equation (25)

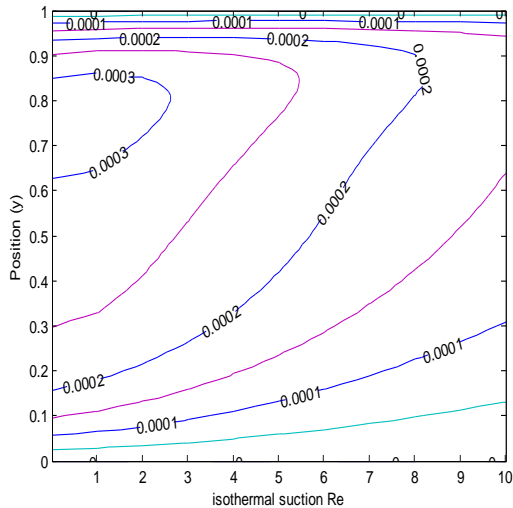


Figure 20: Contour graph of temperature $\theta(y)$ at various values of suction Re with $\beta = 0.04$, $M = 1.0$, $Br = 0.3$, $Pe = 7.1$, $Da = 0.1$ (isothermal) for equation (25)

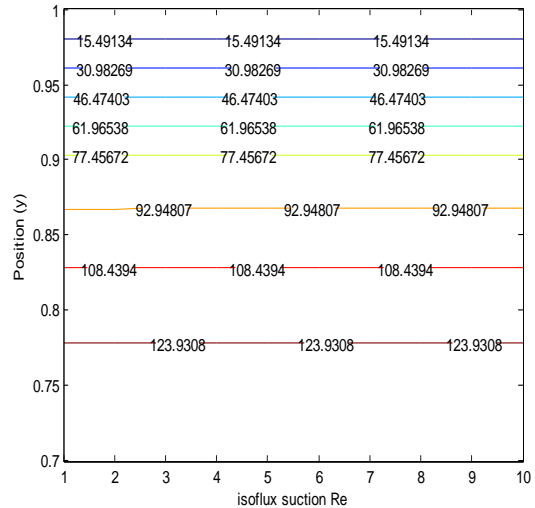


Figure 21: Contour graph of temperature $\theta(y)$ at various values of suction Re with $\beta = 0.04$, $M = 1.0$, $Br = 0.3$, $Pe = 7.1$, $Da = 0.1$ (isoflux) for equation (25)

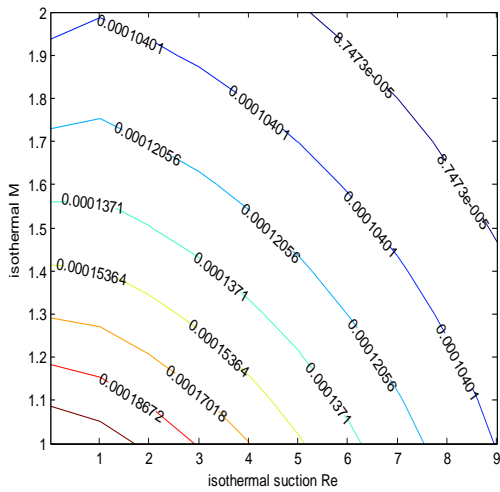


Figure 22: Contour graph of temperature $\theta(y)$ at various values of suction Re and M with $\beta = 0.04$, $Br = 0.3$, $Pe = 7.1$, $Da = 0.1$ (isothermal) for equation (25)

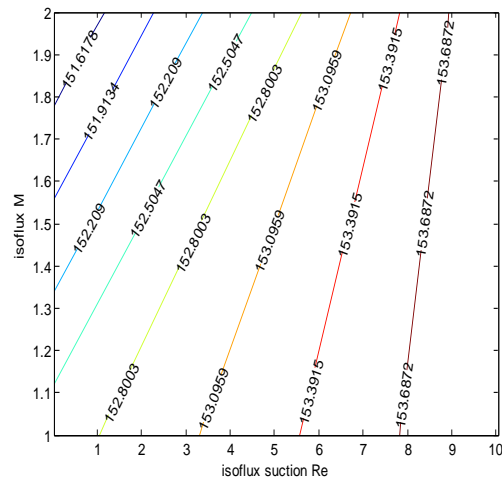


Figure 23: Contour graph of temperature $\theta(y)$ at various values of suction Re and M with $\beta = 0.04$, $Br = 0.3$, $Pe = 7.1$, $Da = 0.1$ (isoflux) for equation (25)